

Quantitative proteomic profiling of tumor-associated vascular endothelial cells in colorectal cancer.

Guoqiang Wang¹, Qiongzi Yang³, Maoyu Li¹, Ye Zhang¹, Yu-xiang Cai³, Xujun Liang¹, Ying Fu¹, Zhefeng Xiao¹, Minze Zhou¹, Zhongpeng Xie², Huichao Huang¹, Yahui Huang³, Yongheng Chen¹, Qiongqiong He^{1,2,3*}, Fang Peng^{1*}, Zhuchu Chen¹

¹ NHC Key Laboratory of Cancer Proteomics, XiangYa Hospital, Central South University, Changsha, Hunan 410008, China

²Department of Pathology, XiangYa Hospital, Central South University, Changsha, Hunan 410008, China

³Department of Pathology, School of Basic Medical, Central South University, Changsha 410008, China

***Corresponding Authors:**

Qiongqiong He, PhD., MD Department of Pathology, XiangYa Hospital, Central South University, Changsha, Hunan 410008, China; Tel: +86-0731-84327291; Fax: +86-0731-84327291; E-Mail:

qiongqionghe@csu.edu.cn

Fangpeng, PhD., NHC Key Laboratory of Cancer Proteomics, XiangYa Hospital, Central South University, Changsha, Hunan 410008, China; Tel: +86-0731-84327239; Fax: +86-0731-84327239; E-Mail: pengfang@csu.edu.cn

Keywords: colorectal cancer, quantitative proteomics, angiogenesis, Tenascin-C.

Summery statement:

We provided large-scale proteomic profiling of vascular endothelial cells in colorectal cancer with quantitative information, a number of potential antiangiogenic targets and a novel vision in the angiogenesis bio-mechanism of CRC.

Summery

To investigate the global proteomic profiles of vascular endothelial cells (VECs) in the tumor microenvironment and antiangiogenic therapy for colorectal cancer (CRC), matched pairs of normal (NVECs) and tumor-associated VECs (TVECs) were purified from CRC tissues by laser capture microdissection and subjected to iTRAQ based quantitative proteomics analysis. Here, 216 differentially expressed proteins (DEPs) were identified and performed bioinformatics analysis. Interestingly, these proteins were implicated in epithelial mesenchymal transition (EMT), ECM-receptor interaction, focal adhesion, PI3K-Akt signaling pathway, angiogenesis and HIF-1 signaling pathway, which may play important roles in CRC angiogenesis. Among these DEPs, Tenascin-C (TNC) was found to upregulated in the TVECs of CRC and be correlate with CRC multistage carcinogenesis and metastasis. Furthermore, the reduction of tumor-derived TNC could attenuate human umbilical vein endothelial cell (HUVEC) proliferation, migration and tube formation through ITGB3/FAK/Akt signaling pathway. Based on the present work, we provided a large-scale proteomic profiling of VECs in CRC with quantitative information, a certain number of potential antiangiogenic targets and a novel vision in the angiogenesis bio-mechanism of CRC.

Introduction

Tumor angiogenesis plays a vital role in creating the tumor microenvironment, and is necessary for tumor growth and metastasis. Currently, angiogenesis inhibitors have become important drugs in the treatment of solid tumors, including colorectal cancer (CRC) (Lopez *et al*, 2019; Riechelmann & Grothey, 2017). Vascular endothelial cells (VECs), which interact with tumor cells, extracellular matrix, and immune killer cells, form the major components of tumor microenvironment. Recently, antiangiogenic strategies have largely focused on targeting VECs (Liu *et al*, 2016; Liu *et al*, 2015). Tumor-associated VECs (TVECs) undergo phenotypic and epigenetic changes during tumor initiation and progression (Xiong *et al*, 2009). Increasing evidence indicates that proteins are primary targets of therapeutic drugs, and that proteins located in TVECs are potential therapeutic targets against tumor angiogenesis and widely used in screening antiangiogenic drugs (Kalen *et al*, 2009; Sonveaux, 2008).

Proteomics has introduced an effective cancer research method that provides new

opportunities for discovering the therapeutic targets of CRC and for revealing the underlying molecular mechanism of this disease. The proteomics of CRC has been extensively studied (Alvarez-Chaver *et al*, 2018; Peng *et al*, 2016), but relatively few studies have focused on tumor microenvironment, especially the proteome of VECs in CRC. However, the VECs comprises only a relatively small percentage of the total tumor volume. Consequently, an altered VECs expression signature may be easily masked in whole tumor studies. To overcome this limitation, laser capture microdissection (LCM) was exploited to isolate a relatively pure VECs from heterogeneous frozen tumor tissue samples in this study.

We compared protein expression in VECs isolated by LCM from CRC tumors and matched adjacent nonmalignant colorectal (ANC) tissues from the same patient. This approach has the advantage of eliminating some of the inherent heterogeneity between individual patients and between different cell types present in the samples (Johann *et al*, 2010; Unwin *et al*, 2003). The resulting peptides of the enzymatically digested proteins were measured by iTRAQ-based quantitative proteomics. Compared to conventional proteomic technology, this approach possesses many advantages, such as high throughput, high accuracy, high repeatability, and high sensitivity, and it can be used for various types of biological samples (Pierce *et al*, 2008). Based on our data, we presented the proteome of VECs in CRC using LCM technology and quantitative proteomics analysis. These TVECs-related proteins may serve as potential therapeutic targets and increase our understanding of the mechanisms underlying CRC angiogenesis. .

Results

Proteomic profiling of VECs in CRC

We compared the global proteomic profiles of paired TVECs and NVECs in 10 patients with CRC to identify proteins and pathways that may be associated with the CRC angiogenesis. As a result, A total of 2058 nonredundant proteins were repeatedly identified and quantified at a minimum confidence level of 95% (unused ProtScore > 1.3) by triplicate iTRAQ labeling and 2D LC-MS/MS analyses (Supplementary Table S1). A protein density plot was subsequently generated to determine the thresholds for clustering DEPs using the ratios of those quantified proteins (Chakraborty *et al*, 2015). Using 10%, 90% and in-between quantile-based thresholds, averaged ratio-fold changes >1.2129 or < 0.7963 between two cohorts of proteins were

categorized as upregulated and downregulated proteins, respectively (Figure 1A).

A total 216 proteins were found to be differentially expressed, including 119 upregulated proteins and 97 downregulated proteins in TVECs relative to NVECs (Supplementary Table S2). Compared to previous literatures, 45 of the top 100 DEPs (top 50 up- and top 50 down-regulated proteins) have been proved as angiogenesis-related proteins, and 17 of the 45 proteins have been reported or predicted as potential targets for cancer antiangiogenic treatment. These proteins are presented in heatmap format in (Figure 1D). In addition, the top 50 up-regulated proteins that are either secreted or localised in the membrane are highlighted in gray in the heatmap as potential therapeutic targets in TVECs (gene names of the respective proteins are: FBLN5, PRG2, YBX1, CEACAM6, S100A9, THBS1, PCBP2, CANX, P4HB, RPL35A, S100A8, MANF, LRRC59, FTL, TOMM22, ATP6V1D, TNC, BASP1 and RNASE3) (Figure 1D). To some degree, these results indicate that our findings were consistent with previous studies and also make new discoveries.

Bioinformatics Analysis

To obtain a biological view of the identified proteins, a total of 2058 proteins were classified according to cellular compartment levels using the PANTHER GO classification system. Variable cellular compartments cell part (38.8%), organelle (26.4%) and membrane (5.1%) are showed in (Figure 1B). Metascape enrichment analysis, accounting for all the DEPs, demonstrated that processes related EMT, ECM-receptor interaction, focal adhesion, PI3K-Akt signaling pathway, angiogenesis and HIF-1 signaling pathway were over-represented (Figure 1C and Supplementary Table S3). The top 50 upregulated and downregulated proteins mapping to each Metascape enrichment term group are presented in heatmap format in Figure 1D. The subcellular localization of these proteins is also presented in the heatmap. Moreover, Metascape enrichment analysis mapped all the identified proteins to 66 signaling pathways (Supplementary Table S4). Interestingly, the results demonstrated that TVECs exhibited an increased dependence on processes related with focal adhesion, PI3K-Akt signaling pathway, HIF-1 signaling pathway and EMT (Figure 2A, 2B and Supplementary Figure S1, Table S5), which might play an important role in CRC angiogenesis.

Validation of the expression of TNC in VECs using immunohistochemistry

In our study, we found TNC was involved in focal adhesion, PI3K/Akt signaling pathway and EMT. To confirm the expression and location of TNC in CRC tissues, we detected the

expression of TNC using immunohistochemistry in 30 cases of NCM, 30 cases of AD, 30 cases of CIS and 50 cases of ICC. As shown in Figure 3 and Table 1, the expression levels of TNC were progressively increased in the CRC carcinogenic process from early stage, AD, to late stage, ICC. ($P < 0.05$). Strong TNC immunostaining was readily detected in the stoma and VECs of the CIS and ICC (Figure 3A and 3B), whereas weak staining in AD and negative staining in NCM were detected (Figure 3C and 3D). In addition, the expression levels of TNC in VECs of lymph nodes with metastasis were strong compared to those in lymph nodes without metastasis (Figure 3E and 3F). Immunostaining of NCM and ICC for the EC marker CD34 was used as a positive control for VECs (Figure 3G and 3H).

Furthermore, we examined the relationship between the expression levels of TNC and clinicopathological characteristics in the 80 cases of CRC tissues above (30 cases of CIS and 50 cases of ICC). The results showed that TNC expression levels in VECs of CRC were closely correlated with lymph nodes metastasis ($P < 0.05$) and distant metastasis ($P < 0.01$) but had no relation with age or gender ($P > 0.05$; Table 2).

Reduction of tumor-derived TNC inactivate ITGB3/FAK/Akt signaling

Tumor-derived TNC promotes or enhances the process of angiogenesis in different tumor models (Hirata *et al*, 2009; Kawamura *et al*, 2018; Pezzolo *et al*, 2011; Rupp *et al*, 2016), but the mechanistic insight has not been fully elucidated. In our previous study, TNC level is much higher in high metastatic potential CRC cell line SW620 compared to the other four CRC cell lines, particularly in the conditioned medium (Li *et al*, 2016). In the current study, We generated CRC cell line SW620 with knockdown of TNC (Figure 4A and 4B), then collected conditioned media from SW620, SW620/Vector and SW620/shTNC cells and subsequently cultured HUVECs with the conditioned media for 24 h. The results indicated that conditioned media from SW620/shTNC cells reduced the expression of ITGB3, Phospho-FAK Tyr397, Phospho-Akt Ser473 (Figure 4C), however, it did not alter the expression of TNC (Figure 4C). These results demonstrated that tumor-derived TNC has a positive influence on ITGB3/FAK/Akt signaling pathway.

Reduction of tumor-derived TNC impairs tubulogenesis, proliferation and migration of HUVECs in vitro

To further confirm whether TNC has an impact on tubulogenesis activity of HUVECs, we plated HUVECs on matrigel together with conditioned media from SW620, SW620/Vector and

SW620/shTNC cells respectively. As shown in Figure 5A and 5B, when TNC knockdown, the incubation of HUVECs with SW620/shTNC conditioned media resulted in a 60% decrease in the formation of capillary-like structures compared with the tubules formed by HUVECs incubated with SW620 conditioned media, and similar results were obtained in cell proliferation and migration of HUVECs using CCK8, wound-healing and transwell chamber assays (Figure 5C, 5D, 5E, 5F and 5G). Our results suggested that TNC has a positive influence on the proliferation, migration and tubulogenesis of HUVECs.

Discussion

Tumor angiogenesis is a complex process leading to abnormalities in vascular structure and function (Sasaki *et al*, 1991). Similar to vasculature in individual organs, TVECs are tissue-specific, which is mostly depending on the tumor microenvironment (Jin *et al*, 2016). In this study, we compared global proteome profiles of VECs derived from normal and tumor tissues to gain insight into CRC angiogenesis and discover antiangiogenic targets for tumor therapy. A total of 216 DEPs were identified, and then GO analysis and systematic pathway-based enrichment analysis was performed. Among the DEPs, many have been reported or predicted as potential targets for cancer antiangiogenic treatment (see Figure1D and Supplementary Table S4), such as FBLN5 (Albig & Schiemann, 2004), CEACAM6 (Zang *et al*, 2015), S100A9 (Eisenblaetter *et al*, 2017; Zhang *et al*, 2017), THBS1 (Lawler, 2002), CANX (Demeure *et al*, 2016), TNC (Kawamura *et al*, 2018), HSP47 (Wu *et al*, 2016), CTTN (Ramos-Garcia & Gonzalez-Moles, 2018), MMP9 (Gupta *et al*, 2013), TGM2 (Lei *et al*, 2018), S100A7 (Padilla *et al*, 2017), LCN2 (Hu *et al*, 2018), RACK1 (Wang *et al*, 2011), PGK1 (Shichijo *et al*, 2004), EPO (Samoszuk *et al*, 1996), CD74 (Gai *et al*, 2018), GRP78 (Kao *et al*, 2018). For these candidate antiangiogenic targets, our results are consistent with previously published data. Furthermore, the focal adhesion, PI3K-Akt signaling pathway, HIF-1 signaling pathway and EMT were identified as significantly and consistently proangiogenic categories in CRC as these pathway-related proteins were significantly upregulated in TVECs compared to controls.

Focal adhesion is a subcellular structure which acts as a scaffold for many signaling pathways involving integrin or the mechanical force exerted on cells (Shen *et al*, 2018). Many molecules in the focal adhesion complex are implicated in downstream signaling pathways, such

as the AKT1 (Higuchi *et al*, 2013), MAPK/ERK pathway (Ye *et al*, 2017), and Wnt signaling (Yu *et al*, 2012). In this way, pathways impacted by the focal adhesion complex are as varied as apoptosis (Bouchard *et al*, 2008), cell proliferation (Luo *et al*, 2018), cell migration and angiogenesis (Zhao & Guan, 2011). In our findings, the focal adhesion-related proteins were significantly increased in TVECs as compared to controls (Figure 2A), which indicated the focal adhesion pathway may play a crucial role in CRC angiogenesis. Therefore, uncovering the molecular processes underlying focal adhesion hub signaling will foster the development of reasonable and feasible multimodal treatment options towards CRC.

The role of PI3K/Akt signaling pathway and HIF-1 signaling pathway in angiogenesis and tumor progression were well-documented (Karar & Maity, 2011). Hypoxia leads to the stabilization of HIF-1 α and is a major stimulus for tumor cells to increase the expression of VEGF. However, the activation of the PI3K/AKT pathway in tumor cells can also increase VEGF secretion. Moreover, PTEN/PI3K/AKT regulates the proteasome-dependent stability of HIF-1 α under hypoxic conditions and controls tumor-induced angiogenesis and metastasis (Joshi *et al*, 2014). The HIF-1 signaling pathway and PI3K signaling pathway have been exploited for the development of new cancer therapies (Post *et al*, 2004; Tanaka *et al*, 2015; Thorpe *et al*, 2015). In the current study, HIF-1 and PI3K/AKT signaling pathway-related proteins were significantly upregulated in TVECs compared with controls (Figure 2B and Supplementary Figure S1). Those findings indicate that PI3K and HIF-1 inhibitors are excellent candidates for the treatment of CRC.

EMT underlies the progression and metastasis of malignant tumors by enabling cancer cells to depart from their primary tumors, invade surrounding tissues and spread to distant organs. Endothelial-to-mesenchymal transition (EndMT) is often categorized as a specialized form of EMT. Recent studies suggested that EndMT may play a role in angiogenic sprouting by enabling the so-called tip cells, which lead an emerging vascular plexus, to migrate into adjacent tissue (Potenta *et al*, 2008; Welch-Reardon *et al*, 2015). In our study, EMT-related proteins were significantly increased in TVECs as compared to controls (Supplementary Table S5). For example, FBLN5 (fold change=1.81) initiates EMT and enhances EMT induced by TGF-beta in mammary epithelial cells via a MMP-dependent mechanism (Lee *et al*, 2008). Based on the clinical application of anti-angiogenesis therapy in metastatic CRC, the EMT-angiogenesis and EMT

stemness links in the CRC cells, newly synthesized drugs with antiangiogenic/anti-EMT properties could be one of the medications used in the future in the targeted therapy of patients with CRC (Gurzu *et al*, 2016).

In our findings, TNC was implicated in focal adhesion, PI3K/Akt signaling pathway and EMT. Several researchers have demonstrated that TNC promotes neoplastic angiogenesis in various cancers including breast cancer, glioblastoma, and oral and pharyngeal squamous cell carcinoma (Atula *et al*, 2003; Mai *et al*, 2002; Rupp *et al*, 2016). However, few reports have investigated the expression of TNC in VECs of CRC and the mechanism for promoting CRC angiogenesis. In our study, we found that the expression of TNC in VECs correlated with CRC multistage carcinogenesis. This finding suggested that TNC may have a positive effect on CRC angiogenesis and progression. As a following step, we highlighted the role of TNC in triggering ITGB3/FAK/Akt-473 signaling pathway, which promoted HUVEC migration and angiogenesis. Moreover, TNC can be secreted in large amounts by SW620 cells (Li *et al*, 2016), indicating that TNC is more likely to end up in the blood or other body fluids in a ‘measurable’ concentration in CRC patients, which can be used for blood-based diagnostics. Therefore, we demonstrated the potential regulation mechanism of TNC and indicated its possible use as a diagnostic and therapeutic target in CRC.

In conclusion, our study built the first proteome of VECs in CRC and regarded the role of vascular proteins in the process of colorectal angiogenesis. In addition, we demonstrated the function of TNC in regulating ITGB3/FAK/Akt signaling and promoting angiogenesis in human CRC. These findings not only provide the proteomic profiling of VECs in CRC, but also highlight some angiogenesis-related proteins, which may be the potential antiangiogenic targets and suggest new insights into the mechanism of angiogenesis in CRC.

Materials and Methods

Sample collection

Ten fresh-frozen samples of CRC and ten matched ANC tissues were taken from the Department of Surgery, Xiangya Hospital, Central South University, China, and used for iTRAQ labeling. The patients received neither radiotherapy nor chemotherapy before curative surgery and provided a written informed consent form for the study, which was approved by the local ethical

committee. All specimens were obtained from surgical resection and stored at -80°C until further investigation.

An independent set of formalin-fixed paraffin-embedded tissue specimens, namely, 30 cases of nonneoplastic colonic mucosa (NCM), 30 cases of adenomatous colorectal polyps (AD), 30 cases of colorectal carcinoma in situ (CIS) and 50 cases of invasive colorectal carcinoma (ICC), were obtained from the Department of Pathology of the Xiangya Hospital at Central South University and used for immunohistochemical analysis.

Laser capture microdissection

The frozen samples were prepared, stained and diagnosed by pathological examination and a rapid immunohistochemical staining technique was performed in less than 13 min with the DAKO rapid Envision™-HRP system as described (Wu *et al*, 2010). To identify and visualize the VECs in human colorectal tissues for sequential LCM, the specific VEC marker CD31 was used for immuno-staining. After the blood vessels were apparent, the glass slides were replaced with LCM-specific glass slides. The stained areas that had the characteristic morphology of VECs were captured by LCM. LCM was performed with a Leica AS LMD system to purify the cells of interest from each type of tissue as previously described (Cheng *et al*, 2008; Li *et al*, 2012). Each captured cell population was over 95% homogeneous as determined by direct microscopic visualization.

Trypsin digestion and labeling with iTRAQ reagents

To diminish the effects of biological variation on the proteomic results, equal amounts of proteins from ten cases of microdissected samples of CRC and ANC were pooled respectively. Two pooled protein samples were obtained for trypsin digestion and labeled with iTRAQ reagents as follows: CRC, labeled with iTRAQ 116, 117 and 118; ANC, labeled with iTRAQ 113, 114 and 115. The labeled digests were then mixed and dried.

Off-line 2D LC-MS/MS

The mixed peptides were first separated on a strong cation exchange column into ten fractions according to the procedure described in our previous study (Mu *et al*, 2013). Each fraction was dried, dissolved in buffer C (0.1% formic acid, 5% acetonitrile), and analyzed on Q-Exactive systems (Thermo Scientific) in information-dependent mode. Briefly, peptides were separated on reverse-phase columns (EASY column, 10cm, ID 75µm, 3µm, C18-A2) with an Easy

nLC system (Thermo Scientific). Peptides were separated by a linear gradient mobile phase A (5% acetonitrile, 0.1% formic acid) and mobile phase B (95% acetonitrile, 0.1% formic acid) from 5% to 40% of mobile phase B in 60 min at a flow rate of 300 nL/min. Survey scans were acquired from 300-1800 m/z with up to 20 precursors selected for MS/MS and dynamic exclusion for 60s.

Data analysis

The software used for protein identification and quantitation was Proteome Discoverer 1.4 software. The peptide mass tolerance was set at ± 20 ppm and the fragment tolerance mass was set at 0.1 Da. The data analysis parameters were set as follows: Sample type, Itraq 4 plex (peptide labeled); Cys alkylation, MMTS; Digestion, Trypsin; Instrument, Q-Exactive systems; Species, *Homo sapiens*; ID Focus, Biological modifications; Search Effort, Thorough; Max missed cleavages, 2; False discovery rate (FDR) Analysis, Yes; User Modified Parameter Files, No; Bias Correction, Auto; Background Correction, Yes. Identified proteins were grouped by the software to minimize redundancy. All peptides used for the calculation of protein ratios were unique to the given protein or proteins within the group, and peptides that were common to other isoforms or proteins of the same family were ignored.

The average iTRAQ ratios from the triple experiments were calculated for each protein. The confidence level of the altered expression of proteins was calculated by T-test as a P-value, which allows the results to be evaluated based on the confidence level of expression change.

Bioinformatics analysis

The DEPs were first annotated by Gene Ontology (GO) using the PANTHER database (<http://www.pantherdb.org/>). Briefly, GO analysis was used to elucidate the genetic regulatory networks of interest by forming hierarchical categories according to the biological process, cellular component and molecular function aspects of the DEPs. Pathway analysis was performed to examine the significant pathways of the DEPs according to Metascape (<http://metascape.org/gp/index.html#/main>).

Immunohistochemistry

Immunohistochemistry was performed according to the procedure described in our previous study (Zeng *et al*, 2012). Briefly, 4 μ m thick tissue sections were deparaffinized, rehydrated, and treated with an antigen retrieval solution (10 mmol/L sodium citrate buffer, pH 6.0). The sections

were incubated with anti-TNC (1:250; Abcam) or anti-CD34 (1:100; ZSGB-BIO) overnight at 4°C and then incubated with biotinylated secondary antibody followed by addition of avidin-biotin peroxidase. Finally, tissue sections were incubated with 3',3'-diaminobenzidine until a brown color developed, and they were counterstained with Harris' modified hematoxylin. In negative controls, primary antibodies were omitted. The evaluation of immunostaining was performed as previously described (Zeng *et al*, 2012). A score (ranging from 0-6) was obtained for each case. A combined staining score of ≤ 2 was considered to be weak staining (no/low expression), a score between 3 and 4 was considered to be moderate staining (expression), and a score between 5 and 6 was considered to be strong staining (high expression).

Western blotting

For western blot analysis, the same amount (30ug) of whole cell lysate samples or enriched conditioned media samples were subjected to SDS-PAGE and subsequently transferred to PVDF membranes. Membranes were blocked in 5% milk for 2h prior to incubation with primary antibodies against TNC (1:1000; Santa Cruz), ITGB3 (1:1000; Proteintech), FAK Phospho-FAK Tyr397, Akt, Phospho-Akt Ser473 (1:1000; Cell Signaling Technology) overnight at 4°C. ACTB was used as a control for protein loading and was detected using a mouse anti-ACTB antibody (1:2000; Proteintech). Membranes were incubated with the corresponding secondary antibodies, including anti-rabbit and anti-mouse peroxidase (HRP)-linked IgG (1:1000; KPL) for 1h.

Cell culture, cell transfection and conditioned media preparation

Human colon cancer cell lines SW620 and human umbilical vein endothelial cells (HUVECs) were maintained in RPMI-1640 or DMEM medium supplemented with 10% FBS in a humidified chamber with 5% CO₂ at 37°C. SW620 cells and HUVECs were purchased from the Cell Bank of Type Culture Collection of the Chinese Academy of Sciences (Shanghai, China).

SW620 cells were cultured in 6-well plates until reaching 70% of confluency, the cells were transduced with lentiviral shRNA-TNC (GGAGTACTTTATCCGTGTATT) and lentiviral control (Cyagen Bioscience Inc., Guangzhou, China) at an MOI of 20 in the presence of 5 µg/ml polybrene for 24h and treated with 3 µg/ml puromycin for three days. The generated cell clones were tested for shRNA-TNC stable expression.

The untransfected (SW620), empty vector (SW620/Vector) and TNC shRNA plasmid-transfected SW620 (SW620/shTNC) cells were chosen for conditioned media preparation.

Conditioned media were collected as previously described (Li *et al*, 2016). Briefly, approximately 3×10^6 cells were grown to 70% confluency, and the medium was exchanged with serum-free RPMI-1640 medium. Conditioned media were collected 24h after the change of media and stored at -20°C for use. For subsequent experiments, the conditioned media were filtered using a 0.22 µm filter (Millipore) and concentrated using a Millipore centrifugal filter (3kDa). The protein concentration was determined by a standard Bradford protein assay (Thermo Scientific). After conditioned media were removed, the cell monolayer was washed, scraped and lysed in the presence of protease inhibitors. Protein concentration was determined using a Pierce BCA Protein Assay Kit (Thermo Scientific).

HUVEC proliferation assay

The HUVECs were plated at 2×10^3 cells per well in 96-well tissue culture plates and cultured in a 1:1 mixture of 10% FBS complete DMEM and conditioned media (total 200µl). The cells were cultured for 6 days. Every 24h, 20µl of CCK8 (5 mg/ml; Beyotime) was added to the wells, and cells were further incubated for 2h. The absorbance of each well was read with a Bio-Tek Instruments EL310 Microplate Autoreader at 450nm. The CCK8 assay was performed three times in triplicate.

Wound healing assay

Cell migration was determined by scratch wound healing assay. Briefly, cells were grown in a 1:1 mixture of 10% FBS complete DMEM and conditioned media overnight to confluence in a 6-well plate. Monolayers of cells were wounded by dragging a pipette tip. Cells were washed to remove cellular debris and allowed to migrate for 12-24h. Images were taken at 0h and 12h after wounding under the inverted microscope.

HUVEC migration assay

Migration activity was measured by Transwell assay (Corning, 3422). Approximately 5×10^4 HUVECs were added to the upper chamber in 200µl of 1% FBS DMEM medium. The lower chamber contained 250µl of 10% FBS complete DMEM and 250µl of conditioned media. The plates were incubated for 24h at 37°C in 5% CO₂. After incubation at 37 °C for 48h, cells were fixed with 4% paraformaldehyde and stained with 0.5% crystal violet. Each clone was plated in triplicate for each experiment, and each experiment was repeated at least three times.

HUVEC angiogenesis assay

Matrigel (BD Biosciences, 354248) was melted at 4°C, added to 48-multiwell plates (Corning) at 100 µl/well, and then incubated at 37°C for 30 min. HUVECs (4×10^3 cells) were resuspended in a 1:1 mixture of 250µl of 20% FBS complete DMEM and 250µl of conditioned media (total 500µl with 10% FBS). The cells were added to the wells, and after 7h incubation at 37°C, HUVEC tube formation was assessed by microscopy. Each well was imaged under a light microscope. The numbers of branches were calculated and quantified using MacBiophotonics ImageJ software (NIH).

Statistical analysis

All statistical analyses were performed using the SPSS software package (version 13.0; SPSS, Inc.) and Prism 5.0 software (GraphPad). Data are shown as the mean \pm SEM. The difference in TNC protein expression between the two different kinds of tissue (CRC vs. ANC) was analyzed using a linear trend chi-square test. The relationship between TNC expression and the clinicopathological characteristics in patients with CRC was analyzed using the Mann-Whitney U test and linear trend chi-square test. For *in vitro* assays, the data are reported as biological replicates, with technical replicates indicated in the figure legends. Student's t-tests (unpaired, two-tailed) were performed to determine whether a difference between two values was statistically significant, with $P < 0.05$ considered significant. *In vitro* assays were performed in triplicate unless otherwise stated. p values < 0.05 were considered statistically significant (* $p < 0.05$; ** $p < 0.01$; *** $p < 0.001$).

Funding: This work was supported by National Natural Science Foundation of China, No.81602572; National Natural Science Foundation of Hunan Province, No. 2017JJ3485; Health and Family Planning Commission of Hunan Province, No.B20180907.

Acknowledgements

We would like to thank Prof. Hongwei Lv and Prof. Hong Xiang of Third Xiangya Hospital for the introduction to the HUVECs angiogenesis assay.

Conflict of Interest: The authors declare no potential conflicts of interest.

References

- Albig AR, Schiemann WP (2004) Fibulin-5 antagonizes vascular endothelial growth factor (VEGF) signaling and angiogenic sprouting by endothelial cells. *DNA and cell biology* **23**(6): 367-79
- Alvarez-Chaver P, De Chiara L, Martinez-Zorzano VS (2018) Proteomic Profiling for Colorectal Cancer Biomarker Discovery. *Methods in molecular biology (Clifton, NJ)* **1765**: 241-269
- Atula T, Hedstrom J, Finne P, Leivo I, Markkanen-Leppanen M, Haglund C (2003) Tenascin-C expression and its prognostic significance in oral and pharyngeal squamous cell carcinoma. *Anticancer research* **23**(3c): 3051-6
- Bouchard V, Harnois C, Demers MJ, Thibodeau S, Laquerre V, Gauthier R, Vezina A, Noel D, Fujita N, Tsuruo T, Arguin M, Vachon PH (2008) B1 integrin/Fak/Src signaling in intestinal epithelial crypt cell survival: integration of complex regulatory mechanisms. *Apoptosis : an international journal on programmed cell death* **13**(4): 531-42
- Chakraborty S, Lakshmanan M, Swa HL, Chen J, Zhang X, Ong YS, Loo LS, Akincilar SC, Gunaratne J, Tergaonkar V, Hui KM, Hong W (2015) An oncogenic role of Agrin in regulating focal adhesion integrity in hepatocellular carcinoma. *Nature communications* **6**: 6184
- Cheng AL, Huang WG, Chen ZC, Peng F, Zhang PF, Li MY, Li F, Li JL, Li C, Yi H, Yi B, Xiao ZQ (2008) Identification of novel nasopharyngeal carcinoma biomarkers by laser capture microdissection and proteomic analysis. *Clinical cancer research : an official journal of the American Association for Cancer Research* **14**(2): 435-45
- Demeure K, Fack F, Duriez E, Tiemann K, Bernard A, Golebiewska A, Bougnaud S, Bjerkvig R, Domon B, Niclou SP (2016) Targeted Proteomics to Assess the Response to Anti-Angiogenic Treatment in Human Glioblastoma (GBM). *Molecular & cellular proteomics : MCP* **15**(2): 481-92
- Eisenblaetter M, Flores-Borja F, Lee JJ, Wefers C, Smith H, Hueting R, Cooper MS, Blower PJ, Patel D, Rodriguez-Justo M, Milewicz H, Vogl T, Roth J, Tutt A, Schaeffter T, Ng T (2017) Visualization of Tumor-Immune Interaction - Target-Specific Imaging of S100A8/A9 Reveals Pre-Metastatic Niche Establishment. *Theranostics* **7**(9): 2392-2401
- Gai JW, Wahafu W, Song L, Ping H, Wang M, Yang F, Niu Y, Qing W, Xing N (2018) Expression of CD74 in bladder cancer and its suppression in association with cancer proliferation, invasion and angiogenesis in HT-1376 cells. *Oncology letters* **15**(5): 7631-7638
- Gupta A, Zhou CQ, Chellaiah MA (2013) Osteopontin and MMP9: Associations with VEGF Expression/Secretion and Angiogenesis in PC3 Prostate Cancer Cells. *Cancers* **5**(2): 617-38
- Gurzu S, Silveanu C, Fetyko A, Butiurca V, Kovacs Z, Jung I (2016) Systematic review of the old and new concepts in the epithelial-mesenchymal transition of colorectal cancer. *World journal of gastroenterology* **22**(30): 6764-75

- Higuchi M, Kihara R, Okazaki T, Aoki I, Suetsugu S, Gotoh Y (2013) Akt1 promotes focal adhesion disassembly and cell motility through phosphorylation of FAK in growth factor-stimulated cells. *Journal of cell science* **126**(Pt 3): 745-55
- Hirata E, Arakawa Y, Shirahata M, Yamaguchi M, Kishi Y, Okada T, Takahashi JA, Matsuda M, Hashimoto N (2009) Endogenous tenascin-C enhances glioblastoma invasion with reactive change of surrounding brain tissue. *Cancer science* **100**(8): 1451-9
- Hu C, Yang K, Li M, Huang W, Zhang F, Wang H (2018) Lipocalin 2: a potential therapeutic target for breast cancer metastasis. *OncoTargets and therapy* **11**: 8099-8106
- Jin H, Cheng X, Pei Y, Fu J, Lyu Z, Peng H, Yao Q, Jiang Y, Luo L, Zhuo H (2016) Identification and verification of transgelin-2 as a potential biomarker of tumor-derived lung-cancer endothelial cells by comparative proteomics. *Journal of proteomics* **136**: 77-88
- Johann DJ, Jr., Wei BR, Prieto DA, Chan KC, Ye X, Valera VA, Simpson RM, Rudnick PA, Xiao Z, Issaq HJ, Linehan WM, Stein SE, Veenstra TD, Blonder J (2010) Combined blood/tissue analysis for cancer biomarker discovery: application to renal cell carcinoma. *Analytical chemistry* **82**(5): 1584-8
- Joshi S, Singh AR, Zulcic M, Durden DL (2014) A macrophage-dominant PI3K isoform controls hypoxia-induced HIF1alpha and HIF2alpha stability and tumor growth, angiogenesis, and metastasis. *Molecular cancer research : MCR* **12**(10): 1520-31
- Kalen M, Wallgard E, Asker N, Nasevicius A, Athley E, Billgren E, Larson JD, Wadman SA, Norseng E, Clark KJ, He L, Karlsson-Lindahl L, Hager AK, Weber H, Augustin H, Samuelsson T, Kemmet CK, Utesch CM, Essner JJ, Hackett PB, Hellstrom M (2009) Combination of reverse and chemical genetic screens reveals angiogenesis inhibitors and targets. *Chemistry & biology* **16**(4): 432-41
- Kao C, Chandna R, Ghode A, Dsouza C, Chen M, Larsson A, Lim SH, Wang M, Cao Z, Zhu Y, Anand GS, Ge R (2018) Proapoptotic Cyclic Peptide BC71 Targets Cell-Surface GRP78 and Functions as an Anticancer Therapeutic in Mice. *EBioMedicine* **33**: 22-32
- Karar J, Maity A (2011) PI3K/AKT/mTOR Pathway in Angiogenesis. *Frontiers in molecular neuroscience* **4**: 51
- Kawamura T, Yamamoto M, Suzuki K, Suzuki Y, Kamishima M, Sakata M, Kurachi K, Setoh M, Konno H, Takeuchi H (2018) Tenascin-C Produced by Intestinal Myofibroblasts Promotes Colitis-associated Cancer Development Through Angiogenesis. *Inflammatory bowel diseases*
- Lawler J (2002) Thrombospondin-1 as an endogenous inhibitor of angiogenesis and tumor growth. *Journal of cellular and molecular medicine* **6**(1): 1-12
- Lee YH, Albig AR, Regner M, Schiemann BJ, Schiemann WP (2008) Fibulin-5 initiates

epithelial-mesenchymal transition (EMT) and enhances EMT induced by TGF-beta in mammary epithelial cells via a MMP-dependent mechanism. *Carcinogenesis* **29**(12): 2243-51

Lei Z, Chai N, Tian M, Zhang Y, Wang G, Liu J, Tian Z, Yi X, Chen D, Li X, Yu P, Hu H, Xu B, Jian C, Bian Z, Guo H, Wang J, Peng S, Nie Y, Huang N, Hu S, Wu K (2018) Novel peptide GX1 inhibits angiogenesis by specifically binding to transglutaminase-2 in the tumorous endothelial cells of gastric cancer. *Cell death & disease* **9**(6): 579

Li M, Li C, Li D, Xie Y, Shi J, Li G, Guan Y, Li M, Zhang P, Peng F, Xiao Z, Chen Z (2012) Periostin, a stroma-associated protein, correlates with tumor invasiveness and progression in nasopharyngeal carcinoma. *Clinical & experimental metastasis* **29**(8): 865-77

Li M, Peng F, Li G, Fu Y, Huang Y, Chen Z, Chen Y (2016) Proteomic analysis of stromal proteins in different stages of colorectal cancer establishes Tenascin-C as a stromal biomarker for colorectal cancer metastasis. *Oncotarget* **7**(24): 37226-37237

Liu S, Liu J, Ma Q, Cao L, Fattah RJ, Yu Z, Bugge TH, Finkel T, Leppla SH (2016) Solid tumor therapy by selectively targeting stromal endothelial cells. *Proceedings of the National Academy of Sciences of the United States of America* **113**(28): E4079-87

Liu YR, Guan YY, Luan X, Lu Q, Wang C, Liu HJ, Gao YG, Yang SC, Dong X, Chen HZ, Fang C (2015) Delta-like ligand 4-targeted nanomedicine for antiangiogenic cancer therapy. *Biomaterials* **42**: 161-71

Lopez A, Harada K, Vasilakopoulou M, Shanbhag N, Ajani JA (2019) Targeting Angiogenesis in Colorectal Carcinoma. *Drugs* **79**(1): 63-74

Luo X, Guo L, Zhang L, Hu Y, Shang D, Ji D (2018) Bioinformatics analysis of microarray profiling identifies the mechanism of focal adhesion kinase signalling pathway in proliferation and apoptosis of breast cancer cells modulated by green tea polyphenol epigallocatechin 3-gallate.

Mai J, Sameni M, Mikkelsen T, Sloane BF (2002) Degradation of extracellular matrix protein tenascin-C by cathepsin B: an interaction involved in the progression of gliomas. *Biological chemistry* **383**(9): 1407-13

Mu Y, Chen Y, Zhang G, Zhan X, Li Y, Liu T, Li G, Li M, Xiao Z, Gong X, Chen Z (2013) Identification of stromal differentially expressed proteins in the colon carcinoma by quantitative proteomics. *Electrophoresis* **34**(11): 1679-92

Padilla L, Dakhel S, Adan J, Masa M, Martinez JM, Roque L, Coll T, Hervas R, Calvis C, Llinas L, Buenestado S, Castellsague J, Messeguer R, Mitjans F, Hernandez JL (2017) S100A7: from mechanism to cancer therapy. *Oncogene* **36**(49): 6749-6761

Peng F, Huang Y, Li MY, Li GQ, Huang HC, Guan R, Chen ZC, Liang SP, Chen YH (2016) Dissecting characteristics and dynamics of differentially expressed proteins during multistage carcinogenesis of

human colorectal cancer. *World journal of gastroenterology* **22**(18): 4515-28

Pezzolo A, Parodi F, Marimpietri D, Raffaghello L, Cocco C, Pistorio A, Mosconi M, Gambini C, Cilli M, Deaglio S, Malavasi F, Pistoia V (2011) Oct-4+/Tenascin C+ neuroblastoma cells serve as progenitors of tumor-derived endothelial cells. *Cell research* **21**(10): 1470-86

Pierce A, Unwin RD, Evans CA, Griffiths S, Carney L, Zhang L, Jaworska E, Lee CF, Blinco D, Okoniewski MJ, Miller CJ, Bitton DA, Spooner E, Whetton AD (2008) Eight-channel iTRAQ enables comparison of the activity of six leukemogenic tyrosine kinases. *Molecular & cellular proteomics : MCP* **7**(5): 853-63

Post DE, Devi NS, Li Z, Brat DJ, Kaur B, Nicholson A, Olson JJ, Zhang Z, Van Meir EG (2004) Cancer therapy with a replicating oncolytic adenovirus targeting the hypoxic microenvironment of tumors. *Clinical cancer research : an official journal of the American Association for Cancer Research* **10**(24): 8603-12

Potenta S, Zeisberg E, Kalluri R (2008) The role of endothelial-to-mesenchymal transition in cancer progression. *British journal of cancer* **99**(9): 1375-9

Ramos-Garcia P, Gonzalez-Moles MA (2018) An update of knowledge on cortactin as a metastatic driver and potential therapeutic target in oral squamous cell carcinoma.

Riechelmann R, Grothey A (2017) Antiangiogenic therapy for refractory colorectal cancer: current options and future strategies. *Therapeutic advances in medical oncology* **9**(2): 106-126

Rupp T, Langlois B, Koczorowska MM, Radwanska A, Sun Z, Hussenet T, Lefebvre O, Murdamoothoo D, Arnold C, Klein A, Biniossek ML, Hyenne V, Naudin E, Velazquez-Quesada I, Schilling O, Van Obberghen-Schilling E, Orend G (2016) Tenascin-C Orchestrates Glioblastoma Angiogenesis by Modulation of Pro- and Anti-angiogenic Signaling. *Cell reports* **17**(10): 2607-2619

Samoszuk M, Lin F, Rim P, Strathearn G (1996) New marker for blood vessels in human ovarian and endometrial cancers. *Clinical cancer research : an official journal of the American Association for Cancer Research* **2**(11): 1867-71

Sasaki K, Kiuchi Y, Sato Y, Yamamori S (1991) Morphological analysis of neovascularization at early stages of rat splenic autografts in comparison with tumor angiogenesis. *Cell and tissue research* **265**(3): 503-10

Shen J, Cao B, Wang Y, Ma C, Zeng Z, Liu L, Li X, Tao D, Gong J, Xie D (2018) Hippo component YAP promotes focal adhesion and tumour aggressiveness via transcriptionally activating THBS1/FAK signalling in breast cancer. *Journal of experimental & clinical cancer research : CR* **37**(1): 175

Shichijo S, Azuma K, Komatsu N, Ito M, Maeda Y, Ishihara Y, Itoh K (2004) Two proliferation-related proteins, TYMS and PGK1, could be new cytotoxic T lymphocyte-directed tumor-associated antigens of HLA-A2+ colon cancer. *Clinical cancer research : an official journal of the American Association for*

Cancer Research **10**(17): 5828-36

Sonveaux P (2008) Provascular strategy: targeting functional adaptations of mature blood vessels in tumors to selectively influence the tumor vascular reactivity and improve cancer treatment.

Radiotherapy and oncology : journal of the European Society for Therapeutic Radiology and Oncology **86**(3): 300-13

Tanaka T, Li TS, Urata Y, Goto S, Ono Y, Kawakatsu M, Matsushima H, Hirabaru M, Adachi T, Kitasato A, Takatsuki M, Kuroki T, Eguchi S (2015) Increased expression of PHD3 represses the HIF-1 signaling pathway and contributes to poor neovascularization in pancreatic ductal adenocarcinoma. *Journal of gastroenterology* **50**(9): 975-83

Thorpe LM, Yuzugullu H, Zhao JJ (2015) PI3K in cancer: divergent roles of isoforms, modes of activation and therapeutic targeting. *Nature reviews Cancer* **15**(1): 7-24

Unwin RD, Craven RA, Harnden P, Hanrahan S, Totty N, Knowles M, Eardley I, Selby PJ, Banks RE (2003) Proteomic changes in renal cancer and co-ordinate demonstration of both the glycolytic and mitochondrial aspects of the Warburg effect. *Proteomics* **3**(8): 1620-32

Wang F, Osawa T, Tsuchida R, Yuasa Y, Shibuya M (2011) Downregulation of receptor for activated C-kinase 1 (RACK1) suppresses tumor growth by inhibiting tumor cell proliferation and tumor-associated angiogenesis. *Cancer science* **102**(11): 2007-13

Welch-Reardon KM, Wu N, Hughes CC (2015) A role for partial endothelial-mesenchymal transitions in angiogenesis? *Arteriosclerosis, thrombosis, and vascular biology* **35**(2): 303-8

Wu M, Han L, Shi Y, Xu G, Wei J, You L, Chen Y, Zhu T, Li Q, Li S, Meng L, Lu Y, Zhou J, Wang S, Ma D (2010) Development and characterization of a novel method for the analysis of gene expression patterns in lymphatic endothelial cells derived from primary breast tissues. *Journal of cancer research and clinical oncology* **136**(6): 863-72

Wu ZB, Cai L, Lin SJ, Leng ZG, Guo YH, Yang WL, Chu YW, Yang SH, Zhao WG (2016) Heat Shock Protein 47 Promotes Glioma Angiogenesis. *Brain pathology (Zurich, Switzerland)* **26**(1): 31-42

Xiong YQ, Sun HC, Zhang W, Zhu XD, Zhuang PY, Zhang JB, Wang L, Wu WZ, Qin LX, Tang ZY (2009) Human hepatocellular carcinoma tumor-derived endothelial cells manifest increased angiogenesis capability and drug resistance compared with normal endothelial cells. *Clinical cancer research : an official journal of the American Association for Cancer Research* **15**(15): 4838-46

Ye DJ, Kwon YJ, Shin S, Baek HS, Shin DW, Chun YJ (2017) Induction of Integrin Signaling by Steroid Sulfatase in Human Cervical Cancer Cells. *Biomolecules & therapeutics* **25**(3): 321-328

Yu Y, Wu J, Wang Y, Zhao T, Ma B, Liu Y, Fang W, Zhu WG, Zhang H (2012) Kindlin 2 forms a transcriptional complex with beta-catenin and TCF4 to enhance Wnt signalling. *EMBO reports* **13**(8):

750-8

Zang M, Zhang Y, Zhang B, Hu L, Li J, Fan Z, Wang H, Su L, Zhu Z, Li C, Yan C, Gu Q, Liu B, Yan M (2015) CEACAM6 promotes tumor angiogenesis and vasculogenic mimicry in gastric cancer via FAK signaling. *Biochimica et biophysica acta* **1852**(5): 1020-8

Zeng GQ, Zhang PF, Deng X, Yu FL, Li C, Xu Y, Yi H, Li MY, Hu R, Zuo JH, Li XH, Wan XX, Qu JQ, He QY, Li JH, Ye X, Chen Y, Li JY, Xiao ZQ (2012) Identification of candidate biomarkers for early detection of human lung squamous cell cancer by quantitative proteomics. *Molecular & cellular proteomics : MCP* **11**(6): M111.013946

Zhang X, Wei L, Wang J, Qin Z, Wang J, Lu Y, Zheng X, Peng Q, Ye Q, Ai F, Liu P, Wang S, Li G, Shen S, Ma J (2017) Suppression Colitis and Colitis-Associated Colon Cancer by Anti-S100a9 Antibody in Mice. *Frontiers in immunology* **8**: 1774

Zhao X, Guan JL (2011) Focal adhesion kinase and its signaling pathways in cell migration and angiogenesis. *Advanced drug delivery reviews* **63**(8): 610-5

Table 1 TNC expression in multistage of colorectal epithelial carcinogenic vessels

Multistage	Number	TNC			P-value
		Low (0-2)	Medium(3-4)	High (5-6)	
NCM	30	23	6	1	P < 0.0001
AD	30	15	13	2	
CIS	30	4	17	9	
ICC	50	7	16	27	

Notes: P<0.05 by linear trend chi square test, NCM vs. AD vs. CIS vs. IC.

Table 2 Correlation between expression of TNC protein and clinicopathological characteristics of patients with colorectal carcinoma

Item	Number	TNC			P-value
		Low (0-2)	Medium (3-4)	High (5-6)	
Gender					
Male	46	6	18	22	P=0.840
Female	34	5	15	14	
Age					
≥65	43	7	16	20	P=0.655
<65	37	4	17	16	
TNM stages					
CIS	30	4	17	9	P=0.022
I~II	19	4	9	6	
III~IV	31	3	7	21	
Matched lymph nodes					
Metastasis	31	3	12	16	P=0.001

Non-metastasis	49	21	19	9	
----------------	----	----	----	---	--

Notes: P-value determined by linear trend chi square test between TNM stages; P-value determined by Mann-Whitney U test, male vs. female, age ≥ 65 vs. < 65 , metastatic lymph nodes vs. non-metastatic lymph nodes.

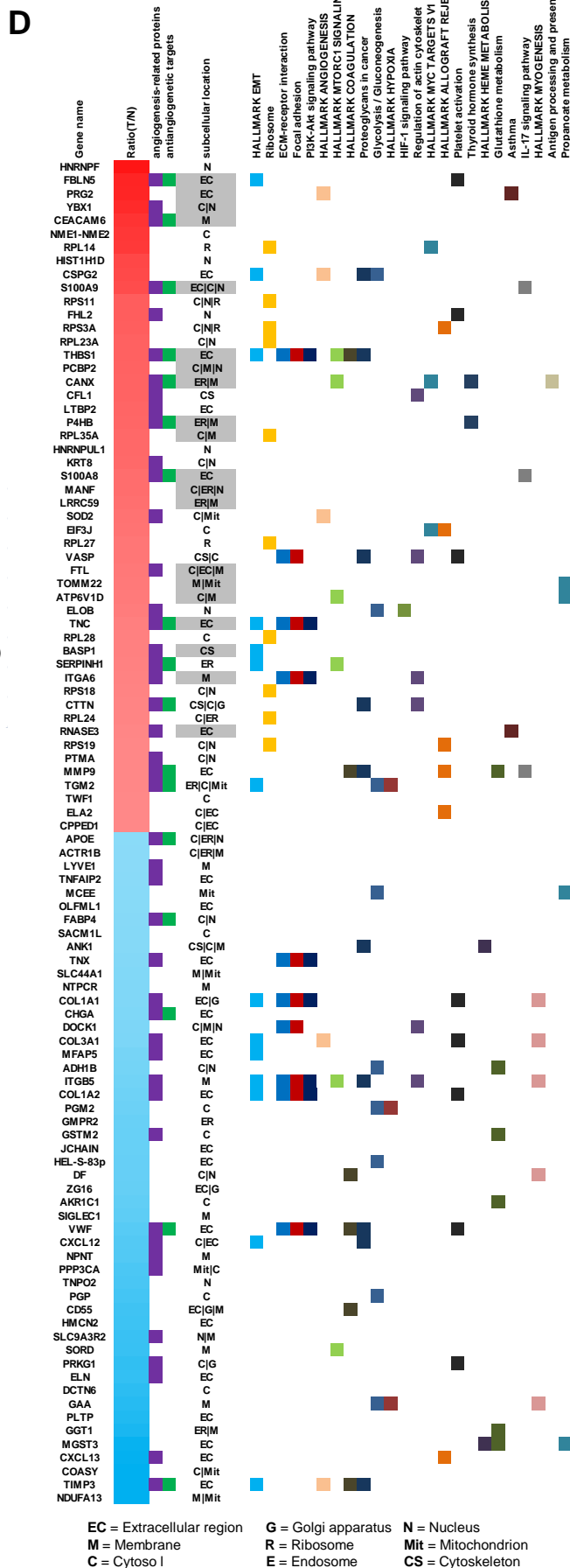
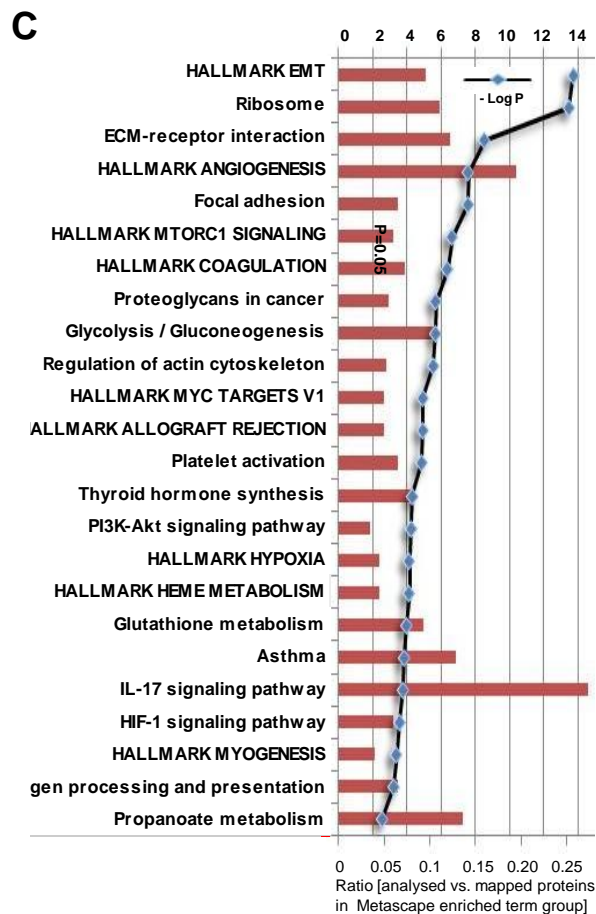
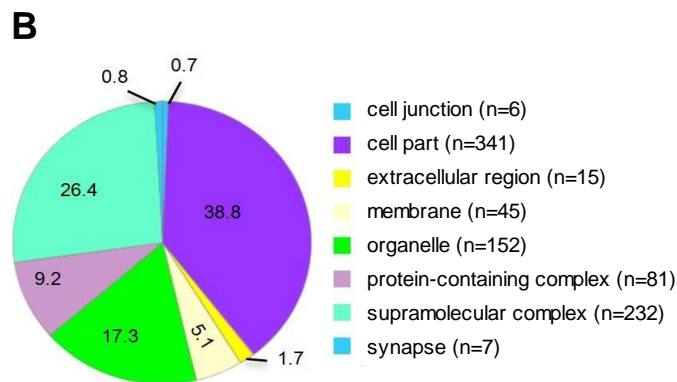
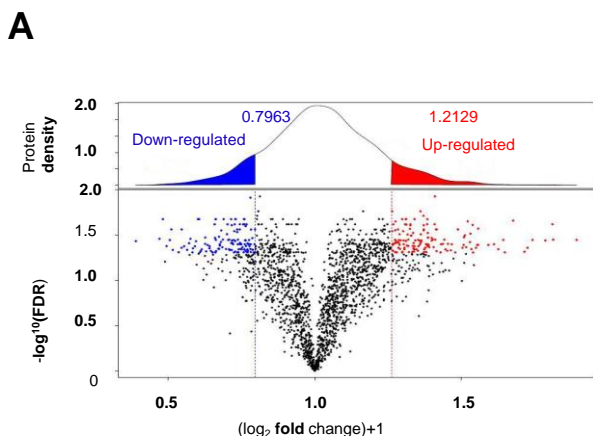
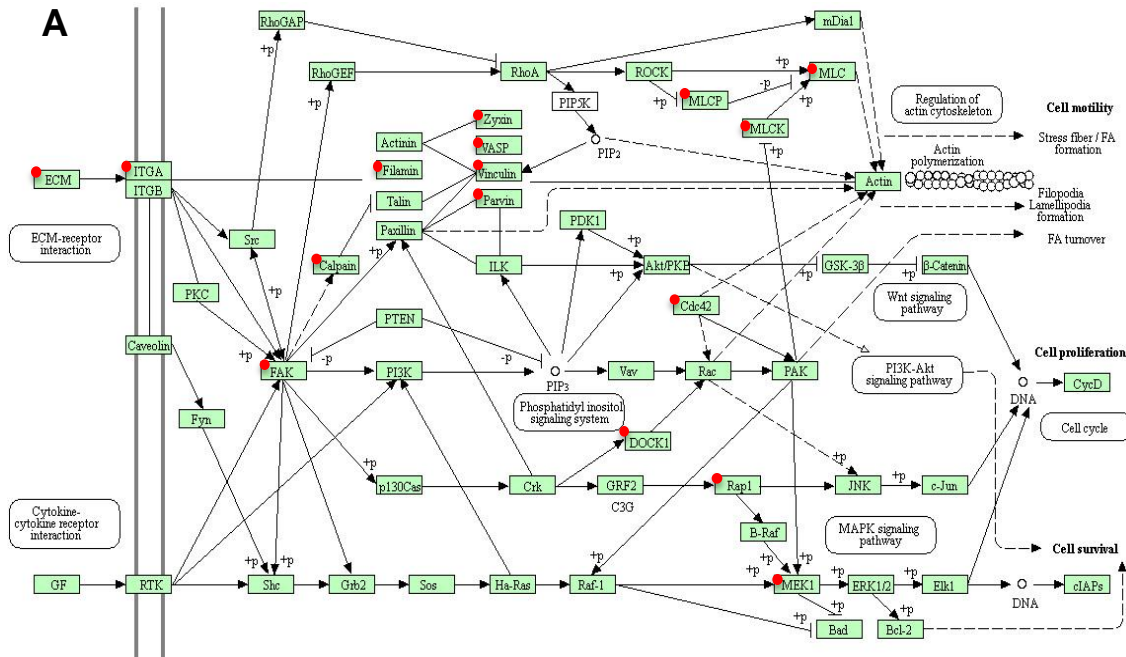


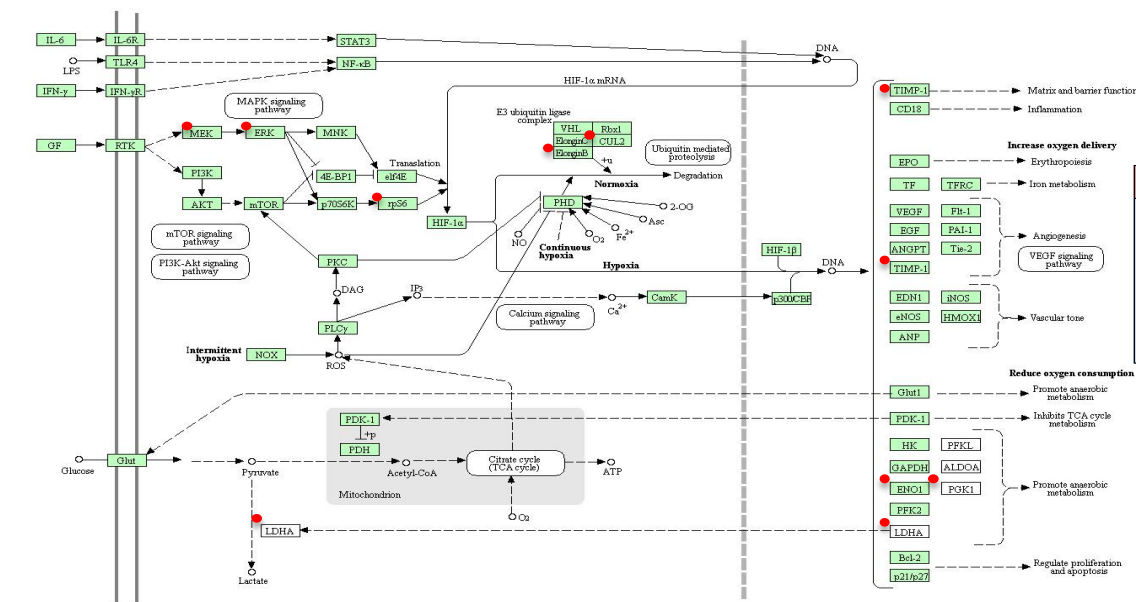
Figure 1: Integrative analysis of identified proteins. (A) The ratio intensity plot representing protein fold change (iTRAQ ratio versus corresponding summed peptide intensity distribution) and protein density plot (upper panel). Red, blue and black clusters indicate up-, down- and unregulated proteins, respectively. (B) A total of 2058 proteins was classified according to the cell components with PANTHER. (C) Metascape pathway analysis mapped the DEPs to 24 signaling pathways. (D) Heatmap of top 50 up- and top 50 down-regulated proteins mapping to each Metascape pathway terms group. The subcellular location of each protein is also presented and up-regulated proteins that are either secreted or membrane are highlighted in gray as potential therapeutic targets.

A



pathway node	ID number	Gene name	Ratio (T/N)
VASP	P50552	VASP	1.45
ECM	A0A024R8	TNC	1.42
ITGA	P23229	ITGA6	1.41
MLCP	P62136	PPP1CA	1.36
Cdc42	P60953	CDC42	1.33
FAK	Q05397	PTK2	1.31
RAC	P15153	RAC2	1.30
MEK1	P19105	MYL12A	1.25
Rap1	P62834	RAP1A	1.22
ECM	P07942	LAMB1	1.21
Rap1	P61224	RAP1B	1.15
Actinin	P12814	ACTN1	1.14
Zyxin	Q15942	ZYX	1.14
Vinculin	A0A024QZ	VL	1.13
Filamin	P21333	FLNA	1.05
DOCK1	B2RUU3	DOCK1	0.70

B



pathway node	ID number	Gene name	Ratio (T/N)
ENO1	P06733	ENO1	1.37
LDHA	P00338	LDHA	1.33
PKG1	P00558	PGK1	1.34
ElonginB	B8ZJ28	ELOB	1.43
TIMP-1	Q5H9A7	TIMP1	1.29
ERK	P27361	MAPK3	0.96
MEK	B4DFY5	MAP2K1	1.23
rpS6	P62753	RPS6	1.19
GAPDH	P04406	GAPDH	1.25
CUL2	Q13617	CUL2	0.95

Figure 2: Focal adhesion pathway (A) and HIF-1 signaling pathway (B) altered in a CRC. Green rectangle with red mark means the identified proteins. Green rectangle without red mark means species-specific enzymes. White rectangle means reference pathway. The solid line indicates molecular interaction. The dot line means indirect effect. The pathway node in the right panel corresponds to the red marked node in the left diagram. ID number is the Swiss-Prot accession number. Ratio (T/N) = Ratio of TVECs to controls.

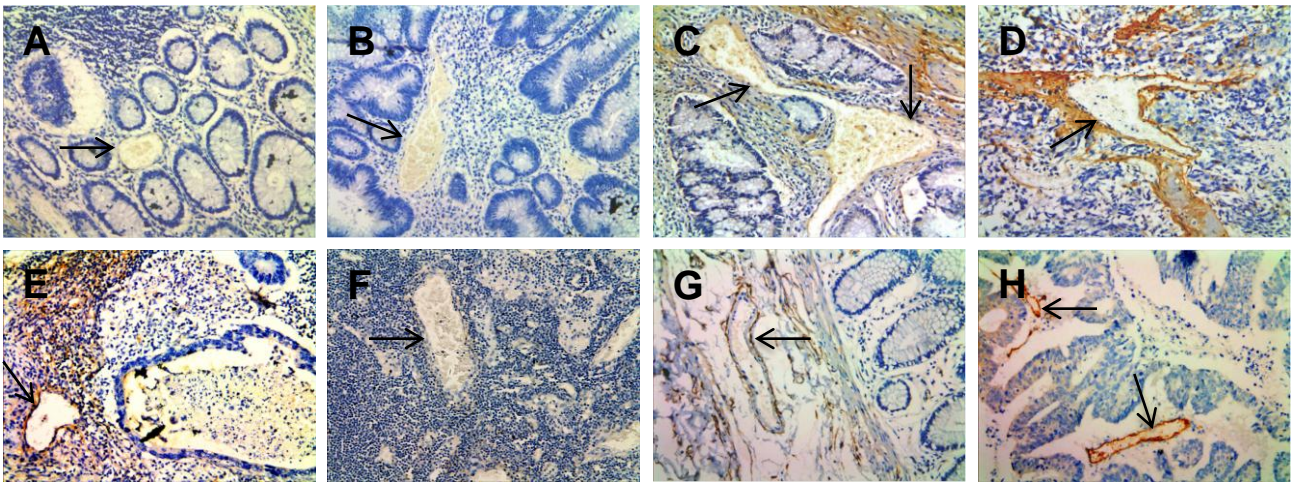


Figure 3: Representative results of immunohistochemistry show the expression of TNC in vessels. Original magnification, $\times 200$. Top panel: TNC immunostaining of NCM (A), ACP (B), CIS (C) and ICC (D). Negative staining was observed in VECs of NCM and ACP, moderate staining in CIS, and strong staining in ICC. Bottom panel: Strong staining was observed in VECs of lymph nodes with metastasis (E). Negative staining was observed in VECs of lymph nodes without metastasis (F). Endothelial cell marker (anti-CD34) immunostaining of NCM (G) and ICC (H).

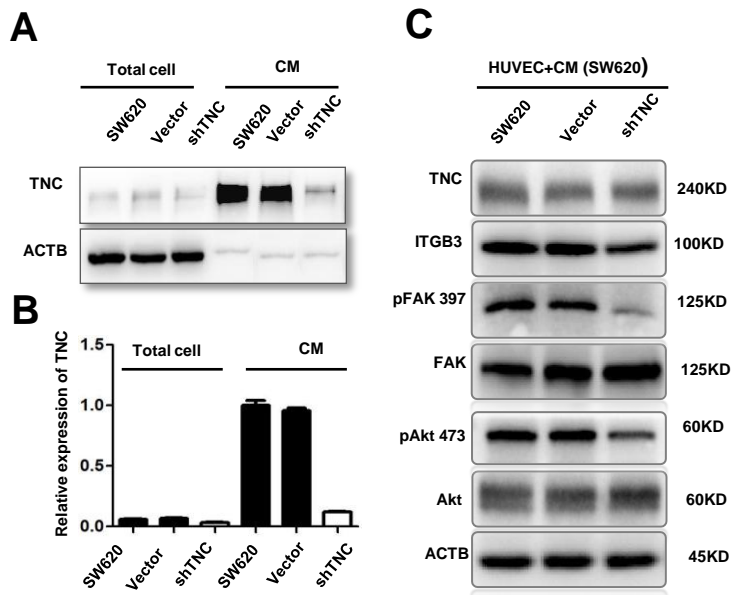


Figure 4: Reduction of tumor-derived TNC inactivate ITGB3/FAK/Akt signaling in HUVECs. (A-B) TNC protein levels in total cell and conditioned medium from untransfected (SW620), empty vector (SW620/Vector) and TNC-shRNA plasmid transfected SW620 cells (SW620/shTNC) were detected by western blot analysis. (C) Treatment with conditioned media (CM) from SW620/sh-TNC cells decreased ITGB3, phosphorylation of FAK-397 and phosphorylation of Akt-473 in HUVECs as compared with CM from untransfected SW620 cells.

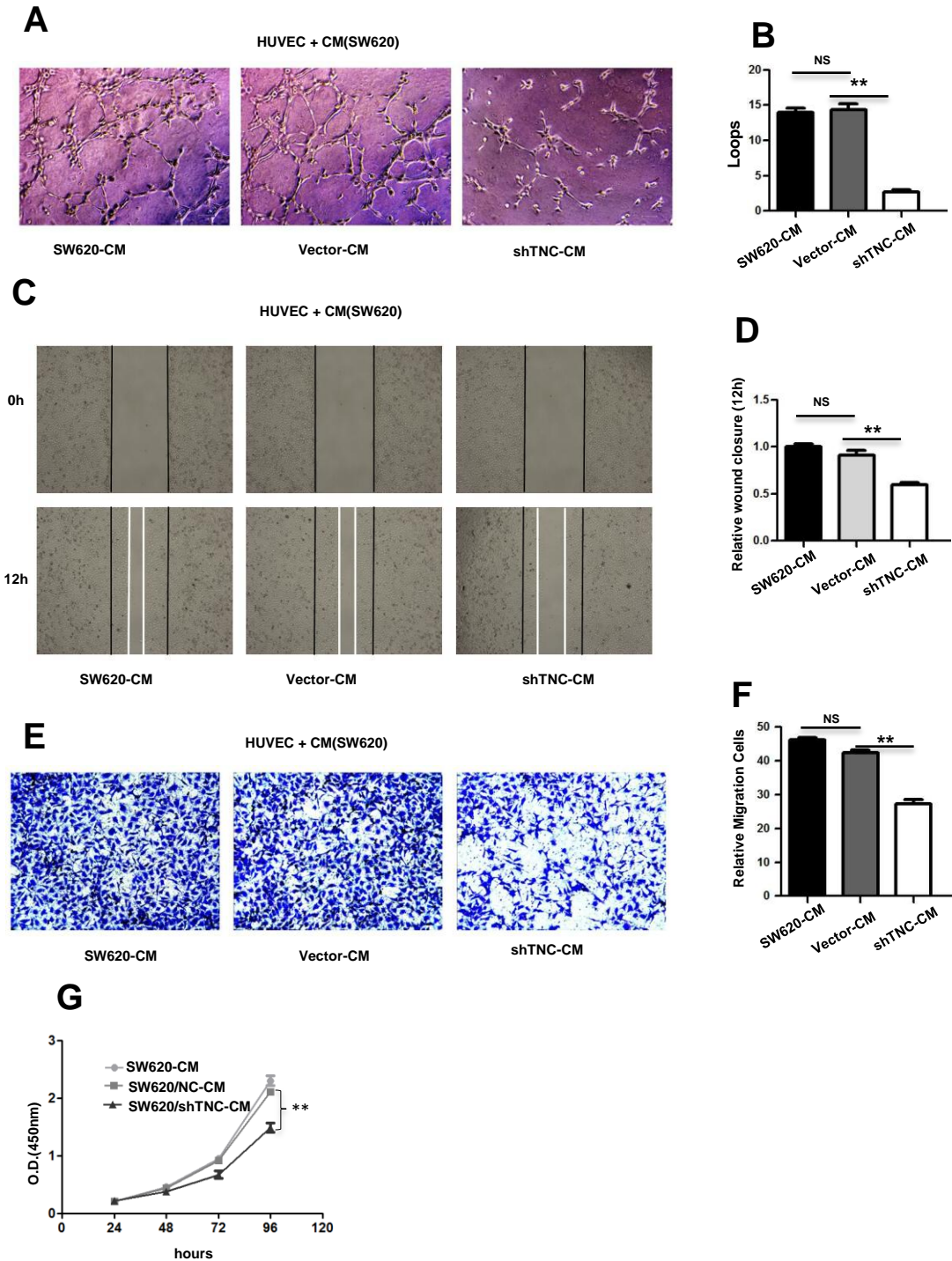


Figure 5: Reduction of SW620-derived TNC leads to the decrease in proliferation, tubulogenesis and migration of HUVECs *in vitro*

(A-B) Representative images (A) of HUVECs 7 h after plating on Matrigel together with conditioned medium from untransfected (SW620-CM) cells and empty vector (Vector-CM)- and TNC-shRNA plasmid-transfected SW620 cells (shTNC-CM) followed by quantification of the number of endothelial closed loops (B). Values are mean \pm SEM from three independent experiments with three replicates.

(C-D) Wound closure of HUVECs at 12 h was quantified upon addition of SW620-CM, Vector-CM and shTNC-CM. Values are the mean \pm SEM from three independent experiments with three replicates.

(E-F) Representative pictures (E) and quantification (F) of HUVEC migration through a transwell chamber containing SW620-CM, Vector-CM and shTNC-CM after 24 h. Values are the mean \pm SEM from three independent experiments with three replicates.

(G) CCK8 assay of HUVECs after treatment with SW620-CM, Vector-CM and shTNC-CM up to 96 h. Values are the mean \pm SEM in HUVECs from three independent experiments with five replicates.